

Evidence for Actin Involvement in Cardiac Z-lines and Z-line Analogues

M. YAMAGUCHI, R. M. ROBSON,* and M. H. STROMER*

*Department of Veterinary Anatomy, The Ohio State University, College of Veterinary Medicine, Columbus, Ohio 43210; and *Muscle Biology Group, Departments of Animal Science, Biochemistry and Biophysics, and Food Technology, Iowa State University, Ames, Iowa 50011*

ABSTRACT Canine and feline cardiac Z-lines and Z-rods were examined by electron microscopy before and after digestion of muscle fibers with Ca^{2+} -activated protease (CAF). Removal by CAF of electron-dense material which covers Z-lines and Z-rods exposed interdigitating longitudinal filaments (6–7 nm in diameter) apparently continuous with thin filaments of the respective I-bands. The newly exposed longitudinal filaments of CAF-treated Z-lines and of CAF-treated Z-rods bound heavy meromyosin and therefore are actin. The width of Z-lines and length of Z-rods are determined by the amount of overlap of actin filaments of opposite polarity. The oblique filaments in Z-lines and Z-rods are responsible for the perpendicular periodicity of Z-lines and Z-rods, and are attributed to α -actinin.

Extensive studies have failed to elucidate the protein composition and structure of Z-lines, mainly because of difficulties in dissecting specifically these highly electron-dense structures. Of the proteins purportedly involved in Z-line structure, substantial evidence has been presented only in the case of α -actinin (15, 32). Contradictory reports on the number and composition of Z-filaments (18, 20, 25, 27), and the mode of attachment to each I-filament (thin filament) (11, 18–22, 25, 28, 34), have been presented. The cause of the diversity of Z-line patterns observed in longitudinal and transverse sections, of I-filament realignment from a hexagonal array near the A-band to a square net near the Z-line, and of variation in Z-line width between fiber types have not been explained.

Cardiac Z-lines, which are wider than those of white and red skeletal muscle (~100, ~50, and ~70 nm, respectively), have been less extensively studied, although similarities in cross-sectional patterns have been reported (10, 13). It is not known how closely the protein composition of cardiac Z-lines resembles that of other muscle types. Anomalous Z-line structures, such as rod bodies (termed "Z-rods" in this paper) in skeletal muscle (24, 26, 33), appear to be directly related in structure and composition to native Z-lines because of their electron-dense appearance, structure, origin, and similar response to proteases. In heart muscle, Z-rods are associated with aging (9, 23) and pathological hypertrophies (1, 3, 29). Because of their large size and high degree of structural order, Z-rods are useful Z-line analogues in studies of the Z-lattice (12).

With the use of Ca^{2+} -activated neutral protease (CAF) (2, 5–7) as a dissecting tool, we have obtained new evidence on

the structure of cardiac Z-lines and Z-rods, on what determines the width of cardiac Z-lines, and on how closely Z-rods are related to Z-lines. The protein composition of Z-filaments is discussed.

MATERIALS AND METHODS

Source of Muscles and Preparation of Glycerinated Muscle: Hearts were obtained from three aged dogs (10, 12, and 14 yr old) and one aged cat (estimated to be more than 12 yr old) after killing the animals with sodium pentobarbital. Samples of papillary and ventricular wall muscles were immediately removed. A portion of the tissue was fixed for electron microscopy as described later; the remainder was teased into small strips and placed in cold phosphate-buffered glycerol (16). 1 mM NaN_3 was added to the solution to prevent bacterial growth. The strips were stored in glycerol for at least 30 d at 0°C with several changes of solution. Before treatment of glycerinated muscle with CAF, strips were further dissected under a dissecting microscope specially equipped with a chilled-ice system to smaller strips which contained approximately 10–20 fibers. These strips were then immersed in several changes of buffered glycerol solution for additional glycerination, and were washed with Tris-acetate buffer solution (see CAF Digestion) before enzymic digestion. Tissues from two young dogs (>2 yr old) and one young cat (2 yr old) were used as controls.

Preparation of Protease (CAF) and CAF Digestion: Purified CAF was prepared by the method of Dayton et al. (6), lyophilized in 36% sucrose, and stored at –70°C. Glycerinated muscle strips were washed several times with a solution which contained 0.1 M KCl, 33 mM Tris-acetate, pH 7.5, 3 mM CaCl_2 , 6.6 mM 2-mercaptoethanol, 0.6 mM NaN_3 , 0.35 M sucrose (Buffer Solution), then incubated with 0.2 ml of 0.05–0.18 mg/ml CAF in 2–3 ml of Buffer Solution at 25°C for ~30 min. The supernatant was removed with a pipette, and the fibers were washed with Buffer Solution at 25°C. Digestion and washing were repeated several times (usually four to five for ~20 min each) to obtain complete digestion. The reaction was stopped by adding EGTA to a final concentration of 10 mM. A portion of the CAF-treated residues was processed for electron microscopy.

Decoration with Heavy Meromyosin: Rabbit skeletal muscle heavy meromyosin (HMM) was obtained by a slight modification of Huxley's (16) method. Residues from CAF digestion were decorated with HMM by mixing an equal volume of HMM (4 mg/ml) in 67 mM potassium phosphate buffer, pH 7.0, with an aliquot of CAF-treated fibers (residue) suspended in the Buffer Solution containing 10 mM EGTA for 1-3 h with occasional gentle stirring at 20°C. Excess HMM was removed by four washings with Buffer Solution which contained 10 mM EGTA; HMM-decorated, CAF-treated fibers were then processed for electron microscopy.

Electron Microscope Observations: Samples were fixed for 2-3 h at 2°C in 2.5% glutaraldehyde, 0.1 M sodium cacodylate, pH 7.4, and postfixed at 2°C in 1% osmium tetroxide in veronal acetate buffer, pH 7.4. During fixation, some samples (especially fresh tissue) were clamped isometrically. Samples were embedded in epon-araldite, and sectioned with an LKB Ultratome III or V (LKB Instruments, Bromo, Sweden) with a diamond knife. Sections were doubly stained with uranyl acetate (5% solution in 100% methanol for 1 h or 2% aqueous solution overnight) and lead citrate, and were examined with a Hitachi H-300 or an RCA EMU 4.

Gel Electrophoresis: Supernatants from CAF digestion were combined and filtered through Whatman #1 filter paper. SDS and 2-mercaptoethanol were added to the filtrate to a final concentration of 1% each, and the sample was heated in boiling water. The filtrate was concentrated by Sephadex G-200 in an 8-mm dialysis tube to a concentration of ~1 mg/ml and then dialyzed vs. 1% SDS, 1% 2-mercaptoethanol, and 20 mM Tris-acetate buffer, pH 7.5. A portion of the residue from CAF digestion was washed with Buffer Solution with KCl replaced by NaCl, then placed on Whatman #1 filter paper and dissected into small pieces. Two ml of 1% SDS, 5 mM 2-mercaptoethanol, and 20 mM Tris-acetate buffer, pH 7.5, were added to ~5 mg of residue, and the mixture was homogenized with a glass homogenizer or a microhomogenizer and boiled. About 10 μ l of the sample was applied to a 7.5% polyacrylamide gel according to Weber and Osborn's method (35). Gels were stained with Coomassie Blue and destained with 50% methanol in 9.2% acetic acid. Individually purified skeletal muscle myofibrillar proteins were used as standards.

Counting CAF-exposed Z-Line or Z-Rod Filaments: The longitudinal filaments exposed in Z-lines ($n = 13$) and Z-rods ($n = 18$) in CAF-treated fibers, each magnified more than 50,000 times, were counted in longitudinal sections independently by three people. Thin filaments were counted near the A-I junction at both ends of the Z-line or Z-rod (the average number on one side being ~60) and then along the perpendicular axis at the center of the Z-line or Z-rod.

RESULTS

Native Cardiac Z-Lines and Z-Rods

The normal appearance of aged cat ventricular muscle is shown in Figure 1a. The distinctive features of cardiac muscle fibers (i.e. branching pattern, richness in mitochondria, and the presence of intercalated disks) are evident. The width of Z-lines is ~110 nm, the sarcomere length is ~2.2 μ m, and the A-band width is ~1.5 μ m. Some abnormal Z-lines often are observed adjacent to normally appearing cells and myofibrils. The abnormal Z-lines expand into one or both of the adjacent sarcomeres in conjunction with Z-line streaming and Z-rod formation (Fig. 1a, inset 1).

Electron-dense Z-rods with a crystalline-like structure often are oriented parallel to the long axis of myofibrils and seem to replace single sarcomeres (Fig. 1a, inset 2). The density of expanded Z-lines and Z-rods is the same as that of normal Z-lines, and direct connection of thin filaments to enlarged Z-

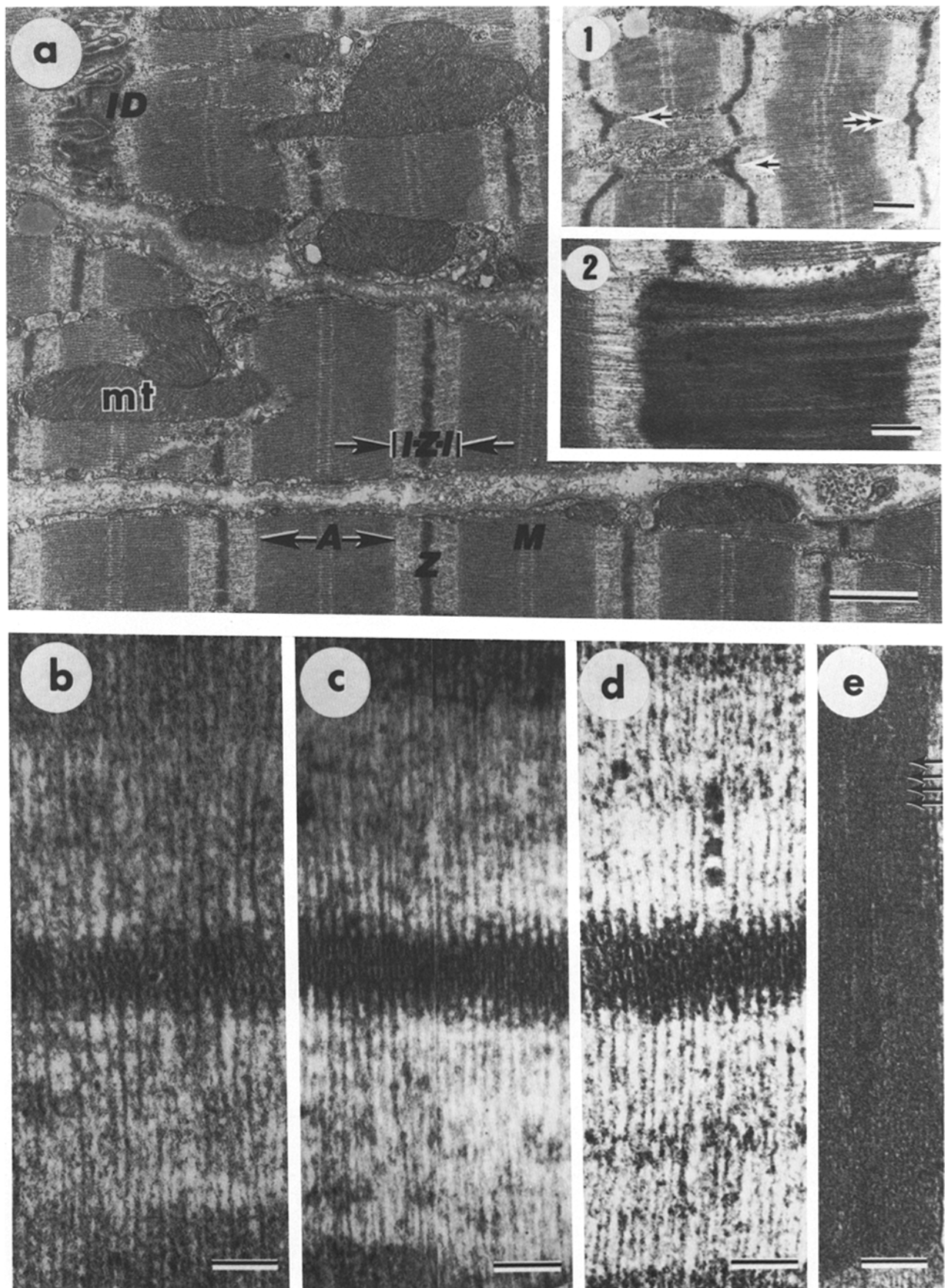
lines can be observed. Although similar Z-line alterations occur both in dog and cat, they were most frequently observed in heart muscle from the 14-yr-old dog.

The width of normal Z-lines is the same in dog and cat myocardium. Among several longitudinal patterns observed in normal Z-lines is the appearance of oblique filaments (oblique filaments will be used throughout this paper to describe the filaments that connect longitudinal filaments and that are responsible for the perpendicular periodicity observed in Z-lines and Z-rods) at various angles (Fig. 1b and c [cat], and d [dog]). The width of Z-lines is constant (100-120 nm) and relatively independent of sarcomere length. The oblique Z-filament angle is, however, directly related to the distance between adjacent I-filaments in a sarcomere on the same side of the Z-line, with greater or larger angles associated with greater distances between adjacent I-filaments. For example, in Fig. 1b, the spacing between I-filaments was 29 ± 3 nm and the Z-filament angle was $32^\circ \pm 5^\circ$, but in Fig. 1d I-filament spacing was 23 ± 5 nm and the Z-filament angle was $20^\circ \pm 3^\circ$. The widths of the I-Z-I regions (the distances between A-I junctions of neighboring sarcomeres) in Fig. 1b, c, and d are 0.7, 0.81, and 0.87 μ m, respectively. This suggests that the space or distance between I-filaments at their insertion into the Z-line is inversely related to sarcomere length, although the effect of sarcomere length on the precise angle of the oblique filaments has not been determined. The I-filaments seem to be directly inserted into the Z-line, and filaments continuous with I-filaments (thin filaments) from opposing sarcomeres interdigitate in the Z-line (Fig. 1b, c, and d). Z-rods from aged canine heart (Fig. 1e) show both a perpendicular periodicity (arrows) and intermittent longitudinal filaments that are continuous with I-filaments.

Effect of CAF on Cardiac Z-Lines

Glycerination by itself does not alter the basic structure of Z-lines or Z-rods (8, 36). Z-lines of glycerinated dog heart muscle partially digested with CAF are shown in Fig. 2. The dense material has been partially removed and longitudinal filaments ~7 nm in diameter are exposed (Fig. 2a and b). Some of the dense covering material removed from Z-lines appears to be scattered in the I-band region on both sides of the Z-line. Fig. 2b shows a higher magnification of the upper right Z-line shown in the inset to Fig. 2b. Filaments entering from opposite sides of the Z-line interdigitate and terminate at the black and white arrows. Widths of I-Z-I regions in Fig. 2a and b are 0.8 and 0.9 μ m, respectively. The ratio of I-Z-I/A-band lengths in Fig. 2b was approximately 0.62. CAF digestion has no noticeable effect on the A-band, and the M-line remains essentially intact. Removal of the dense material covering the Z-line coincides with the disappearance of the oblique filaments. Although some of the exposed filaments are relatively straight, loss of the material lending lateral support to the

FIGURE 1 (a) Longitudinal section of aged (12-yr-old) cat myocardium showing the branching pattern of muscle fibers. (M) M line. (Z) Z-line. (A) A-band. (I-Z-I) Z-line and adjacent I-band regions. (ID) Intercalated disk. (mt) Mitochondrion. Bar, 1.0 μ m. $\times 16,500$. (Inset 1) Z-line anomalies initiate with expansion into one (single arrows) or both (doublet arrows) of the adjacent sarcomeres. Bar, 0.5 μ m. $\times 14,000$. (Inset 2) A Z-rod in dog cardiac muscle with a crystalline-like structure is shown. Rods are continuous with I-filaments. Bar, 0.3 μ m. $\times 30,000$. (b, c, and d) The width of cardiac Z-lines in cat (b and c) and dog (d) is constant (100-120 nm) and seems relatively independent of sarcomere length with no species difference. In all cases, I-filaments seem to be directly connected to the interdigitating filaments in the Z-line region. Oblique filaments are more distinguishable when the perpendicular distance between adjacent I-filaments of the same side of the sarcomere is wider. Bar, 0.1 μ m. $\times 120,000$. (e) The canine Z-rod has perpendicular (arrows) and longitudinal periodicities. Bar, 0.15 μ m. $\times 79,500$.



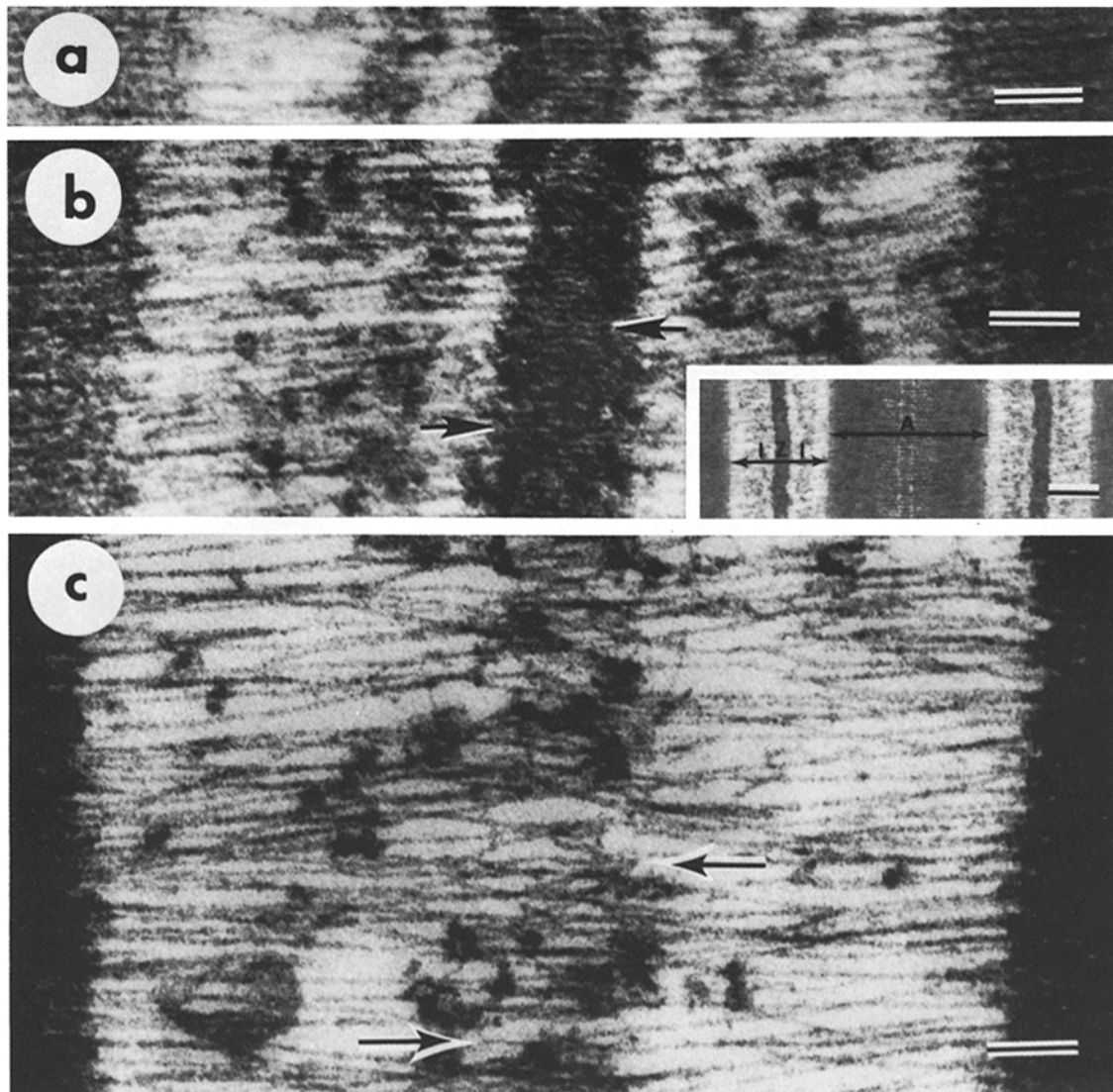


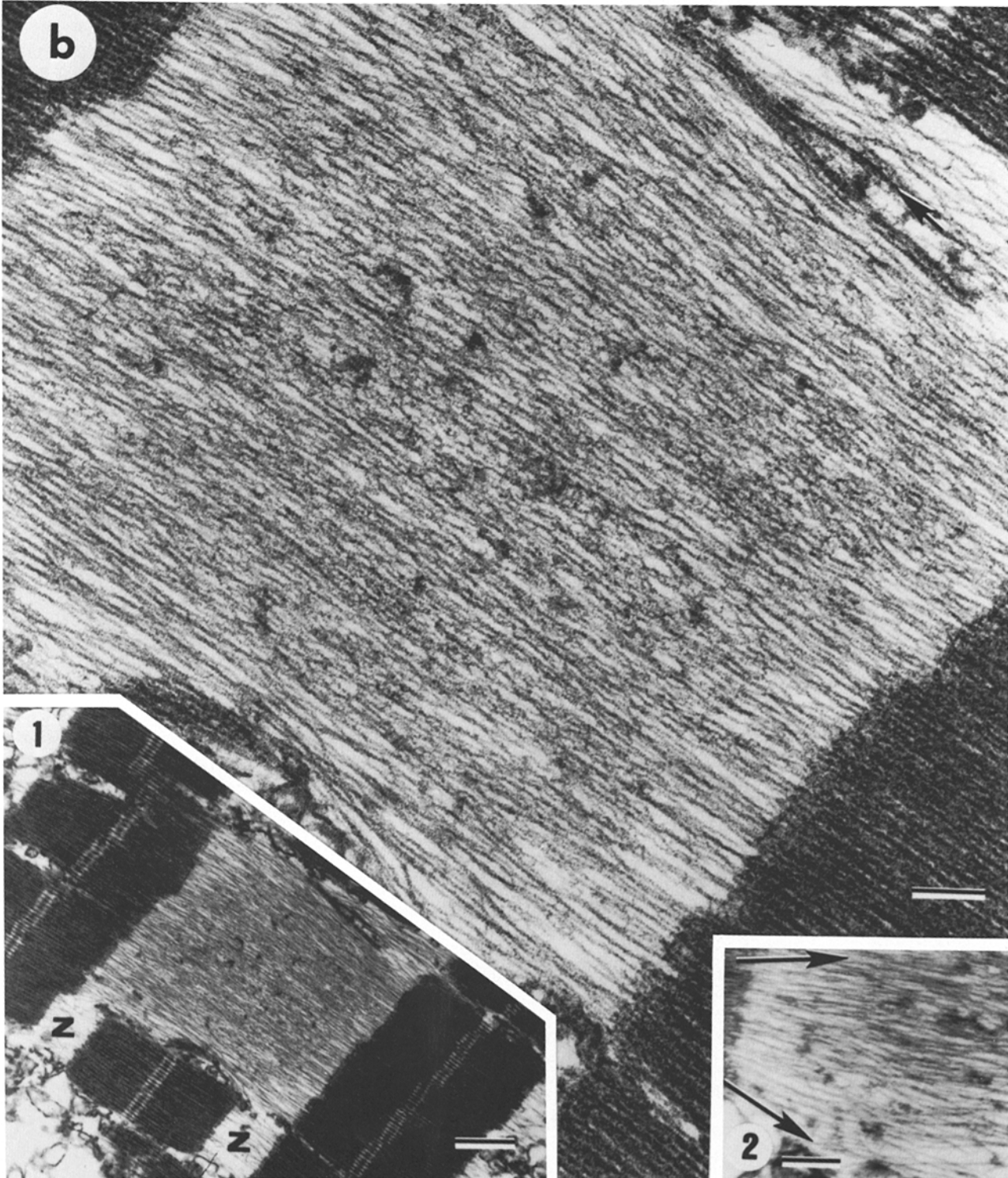
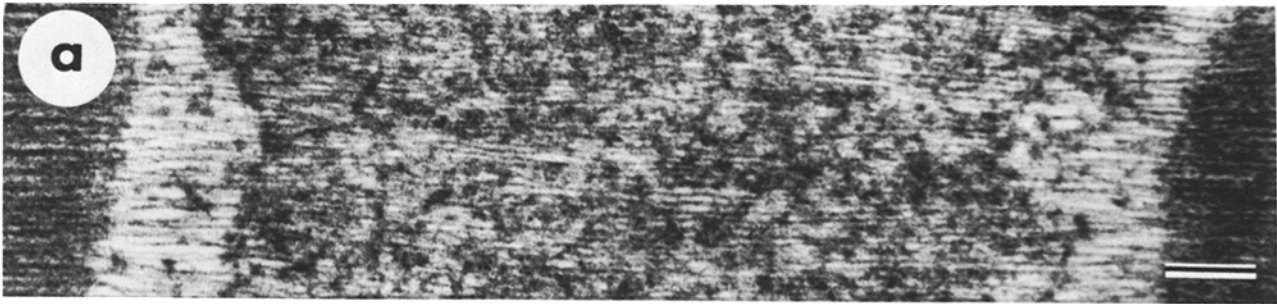
FIGURE 2 CAF-digestion of Z-lines from canine glycerinated cardiac myofibrils. (a) Partially CAF-digested Z-lines show disappearance of oblique filaments and appearance of longitudinal backbone filaments in the Z-line region. Bar, $0.1 \mu\text{m}$. $\times 120,000$. (b) Appearance of interdigitating filaments in the Z-line region. Arrows show termination of exposed filaments. Bar, $0.1 \mu\text{m}$. $\times 120,000$. (Inset) General view of b showing the relaxed sarcomere length of the myofibril after partial CAF digestion. Bar, $0.5 \mu\text{m}$. $\times 14,000$. (c) More prolonged CAF digestion completely exposes a network of filaments (arrows) in the Z-line region. Exposed filaments seem to overlap, and oblique filaments have disappeared. Bar, $0.1 \mu\text{m}$. $\times 120,000$.

longitudinal filaments results in formation of a network of filaments (Fig. 2c) after prolonged CAF digestion. Some termination of filaments can be observed (black and white arrows). CAF-exposed longitudinal filaments in Z-lines clearly overlap. The ratio of the number of longitudinal filaments in CAF-treated Z-lines to the mean number of I-filaments in adjacent sarcomeres was 1.78 ± 0.19 ($n = 13$).

Effect of CAF on Cardiac Z-Rods

Partial CAF digestion reduces the electron density of Z-rods and exposes longitudinal filaments of uniform diameter (6–7 nm) running parallel to the long axis of the myofibril and spanning the lengths of the original Z-rods (Fig. 3a). The original Z-rod in Fig. 3a was $\sim 1.8 \mu\text{m}$ long (see density

FIGURE 3 CAF digestion of Z-rods in canine glycerinated cardiac myofibrils. (a) Partial removal by CAF of dense covering material reveals longitudinal filaments of uniform diameter (6–7 nm) running parallel to the long axis of the myofibril and spanning the lengths of the original Z-rods (see density difference near A-band junction). Bar, $0.2 \mu\text{m}$. $\times 60,000$. (b) More prolonged CAF digestion removes most of the dense material covering Z-rods; oblique filaments disappear, and longitudinal backbone filaments (6–7 nm in diameter) are exposed. The exposed longitudinal filaments are not completely straight because of loss of supporting material perpendicular to their long axis, and they tend to associate with each other. Arrow indicates filaments which resemble myosin filaments. These may be remnants of the A-band in the sarcomere that was displaced by the Z-rod, or alternatively are clumped or superimposed thin filaments. Bar, $0.15 \mu\text{m}$. $\times 82,000$. (Inset 1) General view of the myofibril around the CAF-digested Z-rod. Note the difference of the width between the Z-line and Z-rod regions. Bar, $0.5 \mu\text{m}$. $\times 20,000$. (Inset 2) Exposed longitudinal filaments in a Z-rod sometimes spread laterally (like bristles at the end of a broom, see Fig. 5b). Bar, $0.2 \mu\text{m}$; $\times 48,200$.



differences near A-band regions where edges of Z-rod terminated). The removal of the dense material results in some lateral expansion of the Z-rod and coincides with the disappearance of the perpendicular periodicity present in intact Z-rods. Oblique filaments sometimes observed in Z-rods disappear. The spacing between the exposed longitudinal filaments is not constant; however, the arrangement of these backbone filaments is still fairly straight because of some supporting material left by partial digestion. Prolonged CAF digestion (Fig. 3*b*) removes virtually all dense material covering Z-rods to give a clear view of the backbone filaments. No oblique filaments, occasionally observed in the original Z-rods, are recognizable. The exposed filaments are not as straight as the parallel longitudinal filaments often observed in the original rod (probably because of the loss of supporting material perpendicular to the long axis) and often associates laterally with each other. The myofibril surrounding this Z-rod is contracted (sarcomere length = 1.8 μm ; Fig. 3*b*, inset 1). Thus, the narrow I-band regions between the two edges of the Z-rod and the A-band edges are probably the only areas where there is no overlap of 6- to 7-nm filaments.

Thicker filaments, which appear morphologically to be similar to myosin filaments but may be clumped or superimposed thin filaments, are unaffected by CAF digestion and can be observed occasionally at the edge of Z-rods (Fig. 2*b*, arrow). Some exposed 6- to 7-nm filaments expand into a fan-shaped structure starting near the edge of the A-band (Fig. 3*b*, inset 2). The diameter of these filaments, which are continuous with I-filaments, and their resistance to CAF digestion strongly suggest that they are actin. The measured ratio of filaments at the center of CAF-treated Z-rods to the mean number of I-filaments on either side of rods was 1.62 ± 0.08 ($n = 18$ rods counted).

HMM Decoration of CAF-Digested I-Z-I Region and Z-Rods

HMM decorates I-filaments throughout the I-Z-I region in CAF-treated cardiac muscle (Fig. 4*a*). The I-filaments overlap at the Z-line region. The electron density of the CAF-exposed filaments is enhanced as a result of both HMM binding and the filament overlap at the Z-lines. HMM also binds to all the CAF-exposed longitudinal filaments in the Z-rods to form the well-known arrowhead pattern; thus, the longitudinal 6- to 7-nm filaments in the Z-line proper and those forming the backbone of the Z-rod are actin filaments (Fig. 4*b*). It is difficult to determine the polarity of each exposed filament, but analysis of many sections indicates that where decorated adjacent filaments can be resolved, they have opposite polarity (Fig. 4*c*).

Gel Electrophoresis

Glycerinated, teased cardiac strips, before (Fig. 4*d*, gel 1) and after (isolated residue: Fig. 4*d*, gel 2) CAF treatment, and the material released (Fig. 4*d*, gel 3) by CAF treatment were examined by SDS PAGE. Most of the α -actinin was released by CAF digestion into the supernatant (Fig. 4*d*, gel 3) with minor amounts of other proteins. The major proteins detected in the residues (Fig. 4*d*, gel 2) collected after CAF digestion were myosin and actin. The small amount of desmin (~55-kdalton band) present in cardiac muscle also was degraded by the CAF treatment.

DISCUSSION

Thin filaments from adjacent I-bands enter, and seemingly interdigitate in, the wide Z-line region of cardiac myofibrils (Fig. 1*b-d*). CAF digestion releases electron-dense Z-line material to expose a filamentous backbone. The filamentous appearance of Z-lines revealed by partial digestion by CAF cannot be attributed to additional I-filament-I-filament interaction (i.e., increased insertion of thin filaments into the Z-line region) caused by disruption, because the length of the I-Z-I region and A-band is unaffected by CAF (Fig. 2*b*). The I-Z-I region in Fig. 2*b*, for instance, is 0.9 μm (similar to rest length of 0.81 μm , see Fig. 1*c*). By examining Z-lines in myofibrils undergoing graded degrees of digestion, it was also clear that overlap of interdigitating 6- to 7-nm filaments could be seen while some oblique supporting filaments were still present. In addition, contraction involving I-filament-I-filament interaction has not been documented, and digestion of Z-lines would be expected to weaken rather than increase I-filament interaction. Therefore, it is unlikely that the overlap results from additional intrusion of I-filaments into the Z-line region.

The number of overlapping I-filaments in the Z-line or Z-rod would ideally be twice the number of I-filaments in either adjacent I-band; however, in Z-lines and Z-rods examined in this study, the number of filaments counted averaged 1.6- to 1.8-fold the number in adjacent I-bands. Enumeration of filaments is made difficult by some lateral expansion that occurs during CAF digestion (Fig. 3*b*, inset 2). As illustrated in Fig. 5*b*, spreading of filaments above and below the Z-line region would reduce the chance of counting some filaments; moreover, on prolonged CAF digestion some longitudinal filaments become associated as perpendicular supporting material is lost. Thus, the presence of aggregated (double or triple) filaments likewise decreases the number of filaments counted compared to the predicted number.

The results indicate that the width of Z-lines and Z-rods is determined by the amount of overlap of interdigitating I-filaments. It has previously been postulated (8, 22, 33) that I-(actin)-filaments are the longitudinal filaments of Z-rods. The studies herein showing that the CAF-exposed longitudinal 6- to 7-nm diameter filaments of cardiac Z-lines and Z-rods bind HMM demonstrates they are actin. The origin of Z-rods and their structural similarity to Z-lines in longitudinal section support the view that Z-rods are directly related to native Z-lines and probably are lateral polymers of a basic Z-line unit (12, 33). The close relation between Z-lines and Z-rods was further demonstrated by the similarity of their response to CAF.

In cardiac Z-lines, there are usually three to four sets of oblique filaments responsible for the 40-nm periodicity perpendicular to the long axis of the myofibril. These oblique filaments correspond to Z-filaments that connect opposing interdigitating I-filaments in the Z-lines. If the distance between adjacent I-filaments of the same sarcomere exceeds 22 nm (21) as they enter the Z-line, the oblique filaments form larger angles with the I-(actin)-filaments than if the I-filament spacing is less.

The oblique filaments and the periodic patterns they produce disappear after CAF treatment. Because α -actinin antibodies bind to Z-lines and nemaline rods (17, 30, 31), because of the specificity of CAF in removing undegraded α -actinin from Z-lines (2, 5, 7, 37), and because cardiac and nemaline Z-rods and Z-lines show the same ultrastructural features (8, 9, 13, 14)

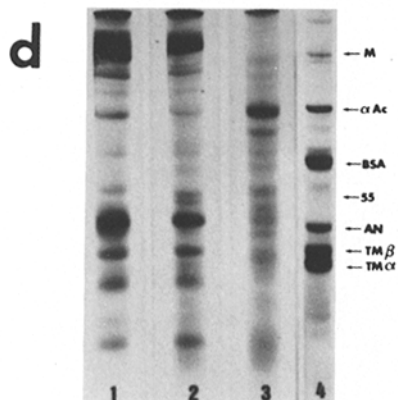
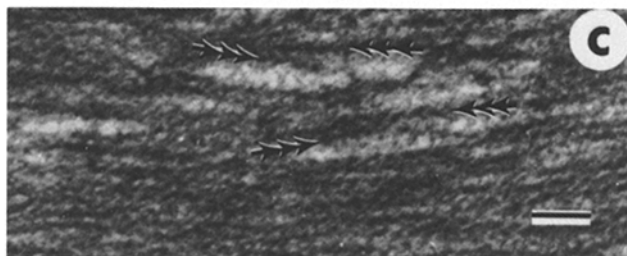
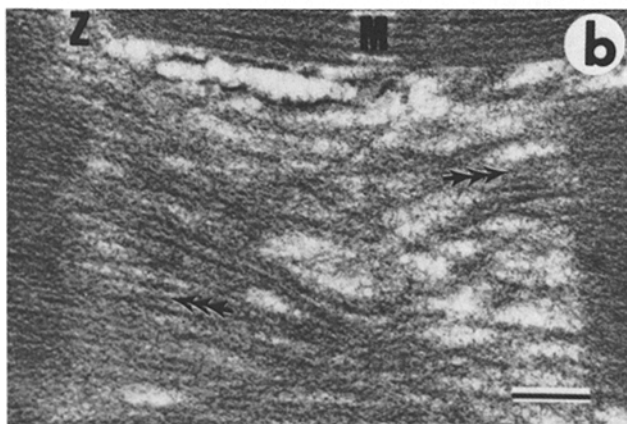
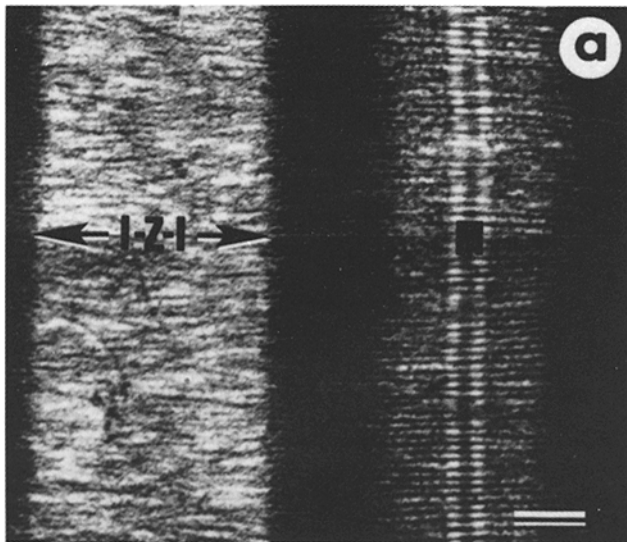


FIGURE 4 HMM decoration of CAF-digested *I-Z-I* region (a) and CAF-digested Z-rods (b and c) from canine samples; electrophoretic pattern of canine cardiac samples before and after CAF digestion (d). (a) In the CAF-digested Z-line region (*I-Z-I*), HMM binds to the I-filaments, which overlap in the center of the Z-line region.

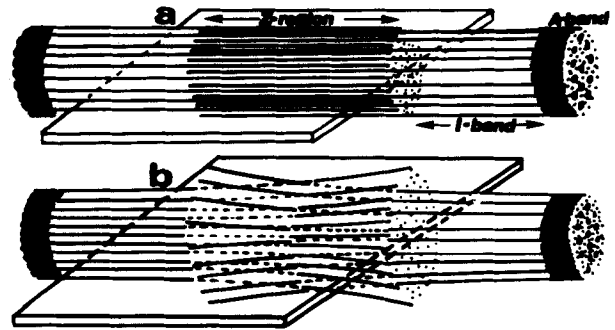


FIGURE 5 Schematic drawing of cardiac myofibrils (*I-Z-I* region) with transecting longitudinal thin sections through the Z-line (or Z-rod) region after CAF digestion. (a) The native state of filaments, which have not spread laterally or associated together after CAF digestion. In this case, the number of exposed filaments in the Z-line after CAF digestion should be twice the number in the adjacent I-band regions. (b) Lateral expansion of CAF-exposed filaments decreases the numbers of filaments counted in the Z-region.

and susceptibility to CAF (37), it seems likely that most of the material removed from cardiac Z-lines and Z-rods by CAF treatment is α -actinin. SDS-gel electrophoresis of the supernatant from CAF digestion of cardiac muscle containing Z-rods shows that the main protein released by CAF is α -actinin (Fig. 4d, gel 3). That α -actinin is responsible for the oblique filaments and the transverse periodicity seen in Z-lines and Z-rods is supported by the disappearance of these features after CAF digestion.

The partial digestion of Z-lines with CAF demonstrates the usefulness of this enzyme for sequentially dissecting and exposing filaments of the Z-line. CAF hydrolyzes purified tropomyosin, troponin T and I, C protein (5) and filamin (4), but has no detectable effect on purified myosin, troponin C, α -actinin, or actin (5). These results are in accord with our structural studies of cardiac muscle that show that thick (myosin) and thin (actin) filaments remain intact after CAF digestion, but that Z-line material (including undegraded α -actinin) is released to expose the underlying filamentous (actin) backbone. Although the use of CAF has allowed us to demonstrate the presence of actin in cardiac Z-lines and Z-rods, we cannot tell from these studies if tropomyosin is associated with the longitudinal actin filaments. Tropomyosin involvement seems likely, however, because the myofibrillar I-filaments are continuous with Z-line and Z-rod longitudinal filaments.

(M) M-line. Bar, 0.5 μ m. \times 39,500. (b) In the CAF-treated Z-rod region, HMM decorates the newly exposed longitudinal filaments. The opposite polarity (arrows) of some of the longitudinal filaments in the rod is clear. Bar, 0.2 μ m. \times 53,000. (c) HMM decoration of CAF-exposed filaments of Z-rods shows that adjacent longitudinal filaments often have opposite polarity (see arrows). Bar, 0.1 μ m. \times 74,000. (d) SDS-gel electrophoretic pattern of proteins from a mixture of glycerinated left ventricular papillary and wall muscles, containing Z-rods, from a 14-yr-old dog. (Lane 1) Glycerinated muscle; (lane 2) residue from CAF digestion; (lane 3) supernatant from CAF digestion; and (lane 4) standards are individually purified myofibrillar proteins isolated from rabbit skeletal muscle, plus bovine serum albumin (BSA). (M) Myosin. (α Ac) α -Actinin. (AN) Actin. (TM α and β) α and β tropomyosin subunits. CAF digestion released most of the α -actinin into the supernatant. The residue after CAF digestion contained mainly myosin and actin with some minor proteins.

The authors wish to thank Ms. M. Shiraya and Mr. T. Nakamura for their excellent technical assistance, and Drs. W. Anderson, R. Wright, T. Fukazawa, T. Wakabayashi, and T. Oda for support in preparing this work.

This work was supported in part by grants from the OSU Canine Research Fund, American Heart Association (AHA) (80-1053), and the Central Ohio Heart Association (81-39) to The Ohio State University and from the Muscular Dystrophy Association National Institutes of Health (HL-15679), and the AHA (79-948; with funds contributed in part by the Iowa Affiliate) to Iowa State University. This is Journal Paper No. J-10437 of the Iowa Agriculture and Home Economics Experiment Station, Ames, Iowa, Projects 2361 and 2127.

Received for publication 9 November 1981, and in revised form 13 August 1982.

REFERENCES

- Bishop, S. P., and C. R. Cole. 1969. Ultrastructural changes in the canine myocardium with right ventricular hypertrophy and congestive heart failure. *Lab. Invest.* 20:219-229.
- Busch, W. A., M. H. Stromer, D. E. Goll, and A. Suzuki. 1972. Ca²⁺-specific removal of Z-lines from rabbit skeletal muscle. *J. Cell Biol.* 52:367-381.
- Cote, G., S. M. Mohiuddin, and P. E. Roy. 1970. Occurrence of Z-band widening in human atrial cells. *Exp. Mol. Pathol.* 13:307-318.
- Davies, P. J. A., D. Wallach, M. C. Willingham, I. Pastan, M. Yamaguchi, and R. M. Robson. 1978. Filamin-actin interaction, dissociation of binding from gelation by Ca²⁺-activated proteolysis. *J. Biol. Chem.* 253:4036-4042.
- Dayton, W. R., D. E. Goll, M. H. Stromer, W. J. Reville, M. G. Zeece, and R. M. Robson. 1975. Some properties of a Ca²⁺-activated protease that may be involved in myofibrillar protein turnover. In *Proteases and Biological Control* E. Reich, D. B. Rifkin, and E. Shaw, editors. Cold Spring Harbor Laboratory, Cold Spring Harbor, New York. 551-577.
- Dayton, W. R., D. E. Goll, M. G. Zeece, R. M. Robson, and W. J. Reville. 1976. A Ca²⁺-activated protease possibly involved in myofibrillar protein turnover. Purification from porcine muscle. *Biochemistry.* 15:2150-2158.
- Dayton, W. R., W. J. Reville, D. E. Goll, and M. H. Stromer. 1976. A Ca²⁺-activated protease possibly involved in myofibrillar protein turnover. Partial characterization of purified enzyme. *Biochemistry.* 15:2159-2167.
- Engel, A. G., and M. R. Gomez. 1967. Nemaline (Z-disc) myopathy: observations on the origin, structure and solubility properties of the nemaline structures. *J. Neuropathol. Exp. Neurol.* 26:601-619.
- Fawcett, D. W. 1968. The sporadic occurrence in cardiac muscle of anomalous Z-bands exhibiting a periodic structure suggestive of tropomyosin. *J. Cell Biol.* 36:266-270.
- Fawcett, D. W., and N. S. McNutt. 1969. The ultrastructure of the cat myocardium. I. Ventricular papillary muscle. *J. Cell Biol.* 42:1-45.
- Franzini-Armstrong, C. 1973. The structure of a simple Z-line. *J. Cell Biol.* 58:630-642.
- Goldstein, M. A., J. P. Schroeter, and R. L. Sass. 1977. Optical diffraction of the Z lattice in canine cardiac muscle. *J. Cell Biol.* 75:818-836.
- Goldstein, M. A., J. P. Schroeter and R. L. Sass. 1979. The Z lattice in mammalian cardiac muscle. *J. Cell Biol.* 83:187-204.
- Goldstein, M. A., M. H. Stromer, J. P. Schroeter, and R. L. Sass. 1980. Optical reconstruction of nemaline rods. *Exp. Neurol.* 70:83-97.
- Goll, D. E., A. Suzuki, J. Temple, and G. R. Holmes. 1972. Studies on purified α -actinin. I. Effect of temperature and tropomyosin on the α -actinin/F-actin interaction. *J. Mol. Biol.* 67:469-488.
- Huxley, H. E. 1963. Electron microscope studies on structure of natural and synthetic protein filaments from striated muscle. *J. Mol. Biol.* 7:281-308.
- Jockusch, B. M., H. Veldman, G. Griffiths, B. A. Vanost, and F. G. I. Jennekens. 1980. Immunofluorescence microscopy of a myopathy- α -actinin is a major constituent of nemaline rods. *Exp. Cell Res.* 127:409-420.
- Kelly, D. E. 1967. Models of muscle Z-band fine structure based on a looping filament configuration. *J. Cell Biol.* 34:827-840.
- Kelly, D. E., and M. A. Cahill. 1972. Filamentous and matrix components of skeletal muscle Z-disks. *Anat. Rec.* 172:623-642.
- Knappeis, G. G., and F. Carlsen. 1962. The ultrastructure of the Z-disc in skeletal muscle. *J. Cell Biol.* 13:323-335.
- Landon, D. N. 1970. The influence of fixation upon the fine structure of the Z-disk of rat striated muscle. *J. Cell Sci.* 6:257-276.
- MacDonald, R. D., and A. G. Engel. 1971. Observations on organization of Z-disk components and on rod bodies of Z-disk origin. *J. Cell Biol.* 48:431-437.
- Munnell, J. F., and R. Getty. 1968. Canine myocardial Z-disc alterations resembling those of nemaline myopathy. *Lab. Invest.* 19:303-308.
- Osame, M., M. Kawabuchi, A. Igata, and H. Sugita. 1975. Experimental nemaline rods induced by anticholinesterase drug (neostigmine methyl sulfate). *Proc. Jpn. Acad.* 51:598-603.
- Reedy, M. K. 1964. The structure of actin filaments and the origin of the axial periodicity in the I substance of vertebrate striated muscle. *Proc. R. Soc. Lond. B. Biol. Sci.* 160:458-460.
- Resnick, J. S., W. K. Engel, and P. G. Nelson. 1968. Changes in the Z-disk of skeletal muscle induced by tenotomy. *Neurology.* 18:737-740.
- Rowe, R. W. D. 1971. Ultrastructure of the Z-line of skeletal muscle fibers. *J. Cell Biol.* 51:674-685.
- Rowe, R. W. D. 1973. The ultrastructure of Z-disks from white, intermediate, and red fibers of mammalian striated muscle. *J. Cell Biol.* 57:261-277.
- Roy, P. E., and P. J. Morin. 1971. Variations of the Z-band in human auricular appendages. *Lab. Invest.* 25:422-426.
- Schollmeyer, J. E., M. H. Stromer, and D. E. Goll. 1972. Alpha-actinin and tropomyosin localization in normal and diseased muscle. *Biophys. J.* 12(2, Pt. 2):280a. (Abstr.)
- Schollmeyer, J. E., D. E. Goll, M. H. Stromer, W. R. Dayton, I. Singh, and R. M. Robson. 1974. Studies on the composition of the Z-disk. *J. Cell Biol.* 63(2, Pt. 2):303a. (Abstr.)
- Stromer, M. H., and D. E. Goll. 1972. Studies on purified α -actinin. II. Electron microscopic studies on the competitive binding of α -actinin and tropomyosin to Z-line extracted myofibrils. *J. Mol. Biol.* 67:489-494.
- Stromer, M. H., L. B. Tabatabai, R. M. Robson, D. E. Goll, and M. G. Zeece. 1976. Nemaline myopathy, an integrated study: selective extraction. *Exp. Neurol.* 50:402-421.
- Ullrick, W. C., P. A. Toselli, J. D. Saide, and W. Phear. 1977. Fine structure of the vertebrate Z-disk. *J. Mol. Biol.* 115:61-74.
- Weber, K., and M. Osborn. 1969. The reliability of molecular weight determinations by dodecyl sulfate-polyacrylamide gel electrophoresis. *J. Biol. Chem.* 244:4406-4412.
- Yamaguchi, M., R. G. Cassens, and D. S. Dahl. 1975. Congenital rod disease: some biochemical aspects of nemaline rods. *Cytobiologie.* 11:335-345.
- Yamaguchi, M., R. M. Robson, M. H. Stromer, D. S. Dahl, and T. Oda. 1978. Actin filaments form the backbone of nemaline myopathy rods. *Nature (Lond.)* 271:265-267.